Journal of Alloys and Compounds, 206 (1994) 31–38
JALCOM 1026

Effects of electrode compacting additives on the cycle life and high-rate dischargeability of $Zr(V_{0.25}Ni_{0.75})_2$ metal hydride electrodes in alkaline solution

Andreas Züttel, Felix Meli and Louis Schlapbach
Institute of Physics, University of Fribourg, CH-1700 Fribourg (Switzerland)

(Received September 17, 1993)

Abstract

Materials used as a compacting agent in the production of metal hydride electrodes influence the electrode performance, *e.g.* cycle life and high rate dischargeability. We have tested several metal hydride electrodes compacted with different metal powders: copper, nickel, cobalt and gold as well as platinum on carbon. The hydrogen storage material of all these electrodes was $ZrV_{0.5}Ni_{1.5}$. The compacted electrodes were cycled in a 6 M KOH electrolyte. Electrodes using nickel as compacting powder showed the best activation, while copper compacted electrodes showed the best cyclic stability. The ratio of compacting material to the active material is also important as it affects the internal resistance of the electrode. This is especially true for an alloy to binder ratio higher than 25 wt.%. Cobalt shows a partly reversible reaction at the standard potential of −0.83 V *vs.* the $Hg/HgO/OH^-$ reference electrode; it can therefore increase the capacity of the cobalt compacted electrode.

1. Introduction

Batteries using AB_2 and AB_5 metal hydride negative electrodes have several advantages, *e.g.* high energy density and long cycle life stability. Reversible alkaline batteries that use metal hydride negative electrodes require a compacting procedure for fabricating the metal hydride electrode because the intermetallic compounds used as the active material are brittle and disintegrate into powder upon hydride formation. The characteristics of the metal hydride electrode can be manipulated by changing the composition of the hydrogen storage alloy. Direct modification of the alloy surface such as micro encapsulation or pretreatments (chemical etching) may also improve the electrodes characteristics, *e.g.* cyclic stability and high rate dischargeability. Microencapsulation of fine particles of the hydrogen storage alloy ($LaNi_5$) with a 1–2 μm thick layer of copper was shown to be very effective in improving the cycle life. The alloy–copper microencapsules, which had dimensions of less than 30 μm, were able to absorb hydrogen easily without special activation and exhibited no decrease in the initial hydrogen storage capacity [1]. Nickel plating of the hydride powder ($Zr_{0.8}Ti_{0.2}Ni_{1.35}$) was also found to increase markedly the durability of the electrodes [2]. Mixing of the metal hydride powder with certain metal oxides, *e.g.* CoO, Co_3O_4 and RuO_2 increased the discharge capacity of $MmNi_{3.6}Mn_{0.4}Al_{0.3}Co_{0.7}$ significantly [3].

The purpose of the present study was to analyze the influence of electrode-compacting material such as copper, nickel, cobalt and gold as well as platinum on carbon on the charge/discharge characteristics of an AB_2 ($ZrV_{0.5}Ni_{1.5}$) metal hydride electrode.

2. Experimental details

The $Zr(V_{0.25}Ni_{0.75})_2$ alloy sample (6 g) was prepared by r.f. levitation melting of appropriate amounts of the constituent elements (Zr 99.8% from Goodfellow GB, V 99.7% from Koch-Light GB, and Ni 99.99% from Johnson Matthey GB), in an evacuated (10^{-6} mbar) water-cooled copper levitation crucible. After holding the sample for 5 min at 1300 °C, the pellet was rapidly quenched to room temperature. The alloy (2 g) was activated under 40 bars hydrogen gas at room temperature. The alloy hydrided within the first 10 min and disintegrated into a powder (grain size 5–50 μm).

For the electrochemical measurements, approximately 20 mg $ZrV_{0.5}Ni_{1.5}$ alloy powder was mixed with one of the following metal powders (approximately 60 mg), copper powder (Merck p.a. <63 μm), nickel

SSDI 0925-8388(93)01026-Z

powder (Merck p.a. <10 μm), cobalt powder (Merck p.a. $\leqslant 1$ μm), gold powder (Metalor filings <100 μm) and carbon powder plated with platinum (Merck 10%Pt/C $\leqslant 100$ μm). The powders were mixed in air and cold pressed (500 MPa) to a pellet ($d=7$ mm). Cycle-life tests were carried out in half-cell experiments in a 6 M KOH electrolyte. A nickel plate was used as counter-electrode in a glass tube separated by a glass filter. The reference electrode was a $Hg/HgO/OH^-$ standard electrode. The working electrodes were charged with a constant current of 5 mA, *i.e.* 250 mA g^{-1} of active material in a 6 M KOH electrolyte. The discharge current was 2.5 mA, *i.e.* approximately 125 mA g^{-1} (the real discharge currents were calculated using the exact weight of active material). The end of discharge potential was -0.6 V with respect to the $Hg/HgO/OH^-$ reference electrode. Every 10 cycles an additional discharge at a tenth of the nominal discharge current was carried out (12 mA g^{-1}). The internal resistance of the electrode was measured on the half-charged electrodes and the equilibrium characteristics of the electrode were measured in special cycles with pulsed charging and discharging (8 mA h g^{-1} per pulse, 3 min resting time).

3. Results

The cycle-life curves of the different compacted electrodes are shown in Fig. 1. These curves were calculated using our previously published model for the cycle life of a metal hydride electrode [4]. The model parameters, *e.g.* the total capacity of the electrode C_{tot}, the active initial capacity C^0_a, the activation constant λ_{act} and the oxidation constant λ_{ox}, were determined by fitting the model to the measured cycle-life curves. They are summarized in Table 1. The total capacity of the electrode C_{tot} represents the capacity of the electrode which it would have without any activation or degradation process. The active initial capacity C^0_a is the calculated active capacity for the electrode on cycle 0; this parameter can be negative if an electrode activates fast and the capacity in the first cycle is small. The activation constant λ_{act} and the oxidation constant λ_{ox} represent the rate of activation and degradation, respectively.

The experiments were performed for up to 150 cycles.

The nickel compacted electrode demonstrates the fastest activation and the highest maximum capacity of 275 mA h g^{-1} at a discharge current of 107 mA g^{-1}. However, this electrode also had the fastest degradation.

There were two copper compacted electrodes, one fixed on the electrode holder with a heat shrink tube, the other one fixed with a special Teflon clip. They show a maximum capacity of 260 mA h g^{-1} with a discharge current of approximately 110 mA g^{-1}. Activation depended on the method of attachment. The electrode fixed with a Teflon clip showed the same activation constant as the nickel compacted electrode, while the heat-treated electrode activated half as fast.

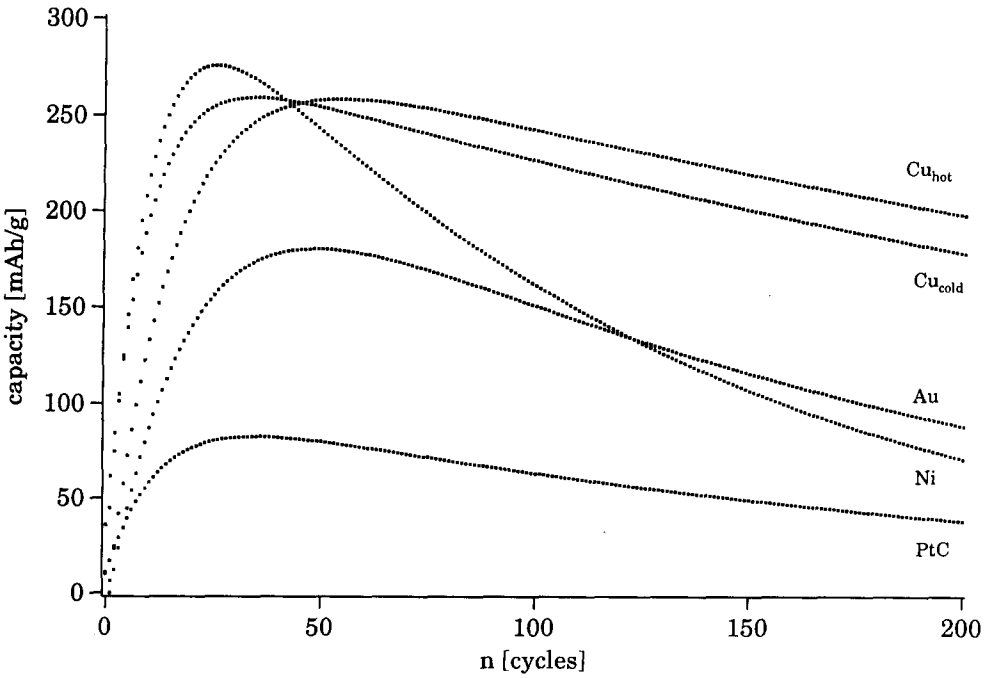

Fig. 1. Cycle-life curves for different compacted $ZrV_{0.5}Ni_{1.5}$ electrodes. The curves were calculated using the fitted parameters of the cycle-life model [4].

TABLE 1. The cycle-life parameters for different compacted electrodes. Discharge current (I_{Dis}), total capacity (C_{tot}), active startup capacity (C_a^0), activation constant (λ_{act}), oxidation constant (λ_{ox}), potential after charge ($-E_{aC}$) and after discharge ($-E_{aD}$) in the equilibrium state of the electrode and the internal resistance (R_i)

Compacted material	I_{Dis} (mA g^{-1})	C_{tot} (mA h g^{-1})	C_a^0 (mA h g^{-1})	λ_{act} (% $cycle^{-1}$)	λ_{ox} (% $cycle^{-1}$)	$-E_{aC}$ (V)	$-E_{aD}$ (V)	R_i (Ωg)
Cu (hot)	118	288	−13	6.7	0.20	0.95	0.81	0.48
Cu (hot)	12	351	−174	11.1	0.11		0.75	
Cu (cold)	102	282	36	11.1	0.24	0.96	0.82	0.45
Cu (cold)	10	350	−567	30.7	0.14		0.76	
Ni	107	3'	11	10.9	0.82	0.96	0.84	0.63
Ni	11		149	20.0	0.60		0.75	
Co	90	o00	580	–	0.43	0.94	0.8	0.72
Co	9	600	580	–	0.43		0.77	
Au	132	233	−13	5.4	0.54	0.96	0.85	0.64
Au	13	313	1	18.4	0.34		0.79	
PtC	115	99	10	8.3	0.51	0.96	0.87	0.76
PtC	12	308	15.6	6.5	0.56		0.82	

The two copper compacted electrodes degraded three times slower than the nickel compacted electrode.

The gold compacted electrode showed a maximum capacity of 176 mA h g^{-1} for a high discharge current of 132 mA g^{-1}. The activation constant was the lowest of the tested electrodes.

The electrode compacted with platinum deposited on carbon showed a maximum capacity of only 80 mA h g^{-1} with the high discharge current of 115 mA g^{-1} and 250 mA h g^{-1} with the low discharge current of 12 mA g^{-1}.

The cobalt compacted electrode shows a very high and constant discharge capacity of 600 mA h g^{-1} independent of the discharge current and cycle number as well. The ratio of high (120 mA g^{-1}) to low (12 mA g^{-1}) rate discharge capacity is a measure of the high rate dischargeability. This value correlates with the internal resistance of the electrode (Fig. 2). From previous measurements of $Zr(V_xNi_{1-x})_2$-alloy electrodes [5] we have found for high resistances (>1 Ω) an almost linear dependency of the high rate dischargeability with the logarithm of the internal resistance.

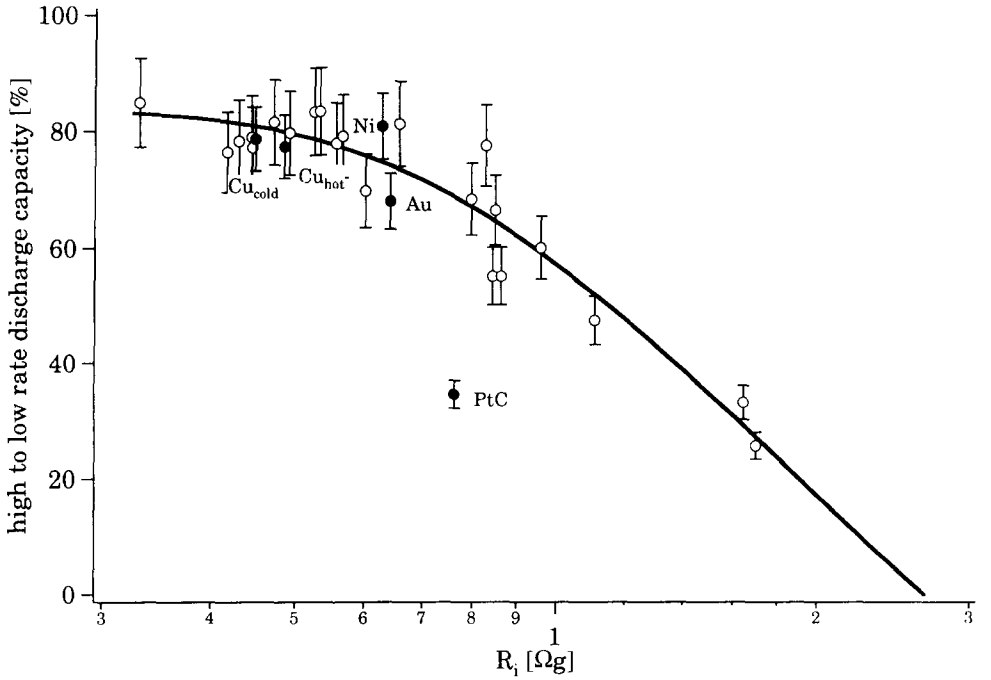

Fig. 2. High to low rate dischargeability as a function of the internal resistance of the electrode. Different compacted $ZrV_{0.5}Ni_{1.5}$ electrodes (●), previous measurements on copper and nickel compacted ZrV_xNi_{2-x} electrodes (○) [5].

For resistances below 1 Ω the curve saturates at a high to low rate discharge capacity ratio of 82%. The internal resistance (R_i) of the electrode was calculated from the overpotential (η) as a function of the applied current (j):

$$R_i = \frac{d\eta}{dj}\left[\frac{mV}{mA \cdot g^{-1}} = \Omega \cdot g\right]$$

The internal resistance of an electrode includes reaction resistance, diffusion resistance and grain-to-grain contact resistance. The applied method allows only an estimation of the sum of all resistances. The dimension of the internal resistance is $\Omega \cdot g$ due to the dimension of currents which are mA g^{-1} because of the unknown active surface area.

Assuming that the electron transfer is rate determining, the Butler–Volmer equation in the linear region of the current j_D as a function of the overpotential η_D ($\eta_D \ll 10$ mV) may be applied:

$$R_D = \frac{d\eta_D}{dj_D} = \frac{R \cdot T}{n \cdot F \cdot j_0}$$

where R is the gas constant (8.314 J K^{-1} mol^{-1}), F the Faraday constant (96 484.56 As mol^{-1}), n the number of transferred electrons and j_0 the exchange current density (mA g^{-1}).

The values of the high rate dischargeabilities of the different compacted electrodes match the curve in Fig. 2 very well, with the exception of the carbon/platinum compacted electrode. The resistance in that case was too low compared with the expected value for high rate dischargeability.

The condition of an electrode is best demonstrated by plotting the potential during a pulsed charge. This is because pulsing allows measurement of the potential of the electrode at the equilibrium state during charge and discharge. Figure 3 shows the potential curve for the copper compacted electrode as a function of the electrode capacity. From this curve we have also calculated the density of states (DoS) for hydrogen in the interstitial sites. This curve allows a better evaluation of the "plateau pressure" on samples which show a sloping plateau. The DoS curve shows two charge maxima due to the hydrogen evolution during charging of the electrode. Figure 4 shows the potential curve of the cobalt compacted electrode. Comparing Fig. 3 with Fig. 4 provides an explanation for the big difference in the discharge capacities of these two electrodes. In addition to the small plateau of the metal hydride at −0.87 V during discharge we found a second large plateau at −0.8 V (potentials were referenced to the $Hg/HgO/OH^-$ electrode).

The equilibrium potential during discharge corresponds to the amount of hydrogen remaining in the alloy. Thus, comparing the potential after discharge with the equilibrium potential allows one to calculate the amount of hydrogen remaining in the electrode. The capacity present after discharge of the nickel compacted electrode was calculated from the difference

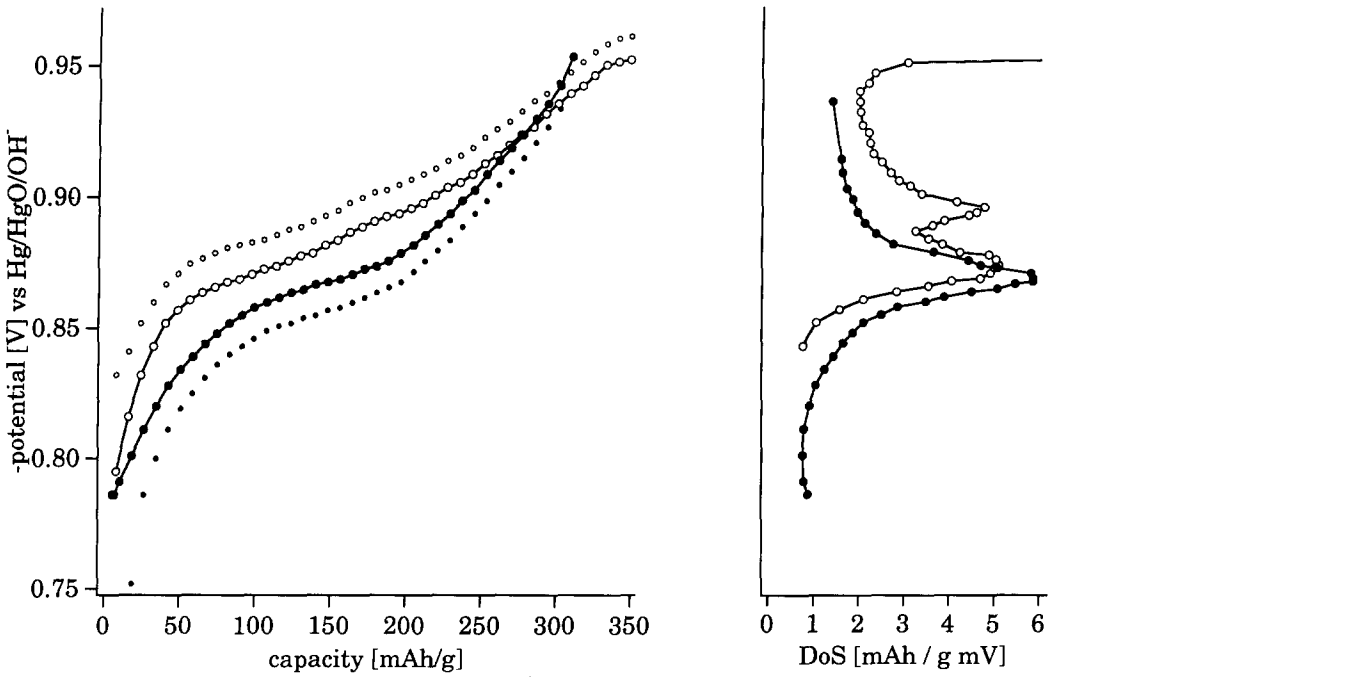

Fig. 3. Equilibrium potential (markers and line) and potential with applied current (25 mA g^{-1}) as a function of the capacity for a copper compacted $ZrV_{0.5}Ni_{1.5}$ electrode (○ for charge and ● for discharge). The calculated density of states for hydrogen at the right-hand side of the figure.

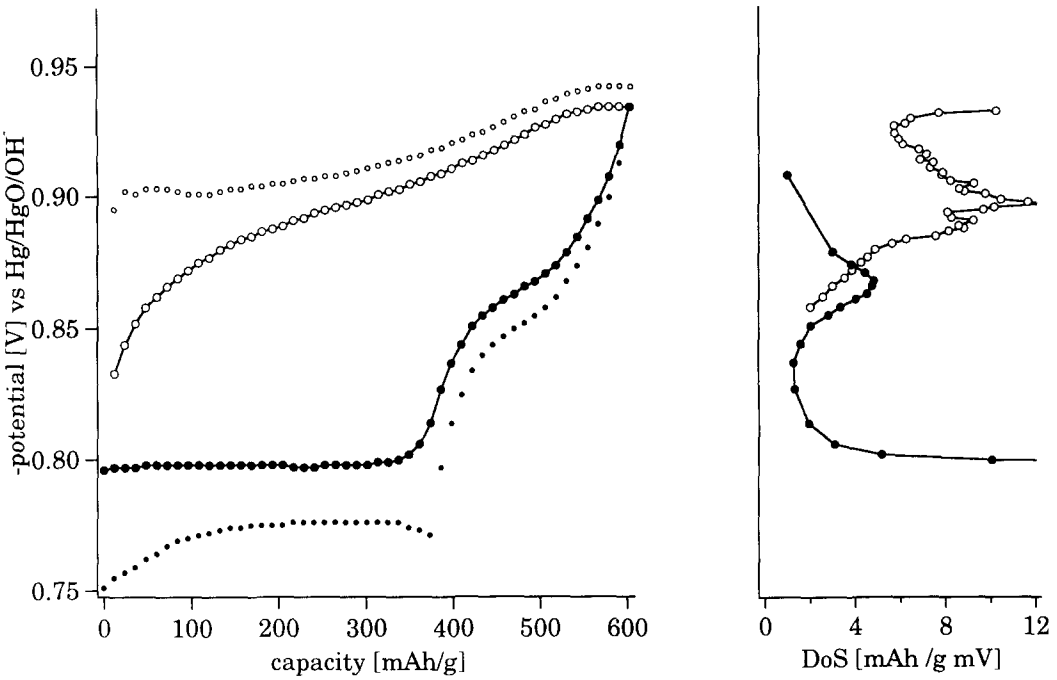

Fig. 4. Equilibrium potential (markers and line) and potential with applied current (25 mA g^{-1}) as a function of the capacity for a cobalt compacted $ZrV_{0.5}Ni_{1.5}$ electrode (○ for charge and ● for discharge). The calculated density of states for hydrogen at the right-hand side of the figure.

between the maximal discharge capacity and the actual discharge capacity for every cycle. The potential after discharge as a function of the remaining capacity is shown in Fig. 5 (open circles). This curve corresponds directly to the equilibrium potential curve (solid circles) during the initial activation of the electrode, *i.e.* for approximately the first 30 cycles. After further cycles the potential after discharge remained at a constant

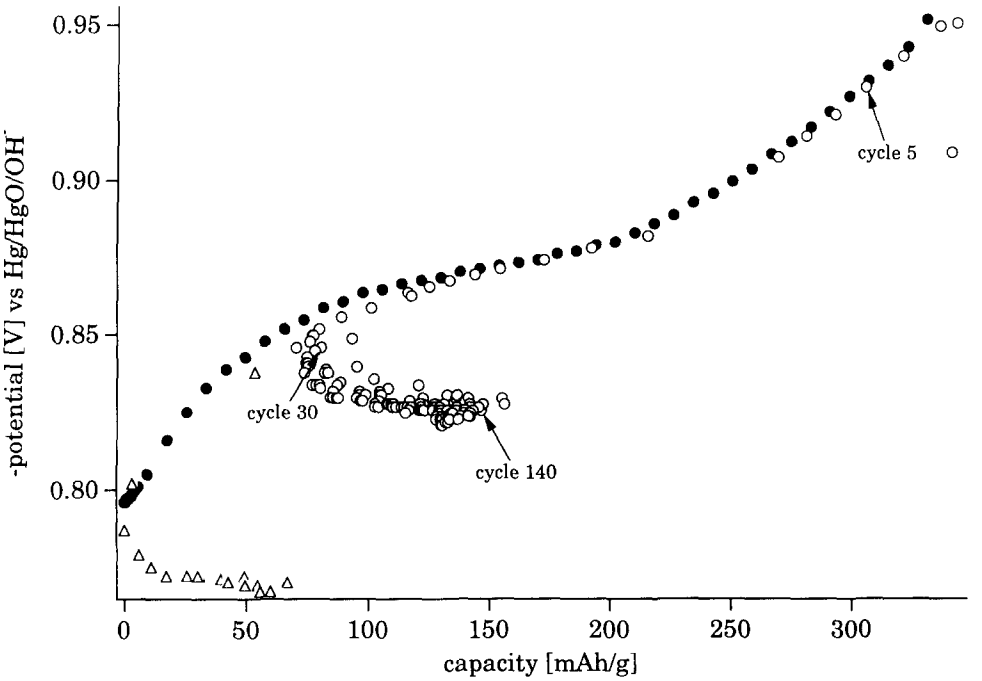

Fig. 5. Equilibrium potential (●) as a function of the capacity for a nickel compacted $ZrV_{0.5}Ni_{1.5}$ electrode. Potential after discharge (○) as a function of the remaining capacity (difference between the maximal capacity and the discharge capacities). Potential after discharge for cycles with an additional discharge at low current (Δ).

TABLE 2. Copper cold compacted electrodes with different alloy to copper ratios (m_{act}/m_{tot}), the internal resistance (R_i), maximum measured capacity (C_{max}) and the high to low rate discharge capacity (C_{hiC}/C_{loC})

m_{act}/m_{tot} (%)	R_i (Ωg)	C_{max} (mA h g^{-1})		C_{hiC}/C_{loC}
		(120 mA g^{-1})	(12 mA g^{-1})	
12.5	0.50	292	374	0.78
25	0.60	274	349	0.78
50	2.0	282	343	0.82

value of approximately −0.82 V *vs.* Hg/HgO/OH^- reference electrode while the discharge capacity decreased, and therefore the calculated hydrogen capacity that remains increased. For the cycles in which there was an additional low rate discharge, the potentials after discharge (triangles) were below the equilibrium potential curve (between −0.77 V and −0.79 V). The calculated remaining capacity also increased with each cycle.

The influence of increasing the ratio of compacting material to active material was tested using copper compacted electrodes. Table 2 summarizes the maximum capacity for high and low rate discharge, the internal resistance of the electrode and the ratio of high to low rate discharge capacities for different alloy to copper powder ratios. The ratio of high to low rate discharge capacities appears to be independent of the relative amount of compacting material. However, the discharge capacity tends to decrease with decreasing copper content. The internal resistance increases with increasing the alloy to copper ratio. Alloy ratios higher than 50% have not been tested because of the inevitable loss of active material during cycling the electrode in our experimental set-up.

4. Discussion

The electrode cycle-life behavior, that is, its reversible capacity, high rate dischargeability, activation and degradation, is strongly dependent on the material with which it is compacted. Cycle-life curves for the two copper compacted electrodes (cold fabricated and heated during fabrication) produced the same maximum discharge capacity and the same degradation constant. However, activation of the electrode fixed with a Teflon clip was twice as rapid as activation of the heat-treated electrode. This effect can be explained by an increase in thickness of the surface oxide layer while heating the electrode in air. From the enthalpies of the oxidation reactions [6, 7] one would assume that the preferred order of vanadium oxide formation would be V_2O_3 and V_2O_4 followed by the oxidation of zirconium to ZrO_2. On the other hand, the thickness of the oxide layer must be very small compared with the grain size because both electrodes achieved the same maximum capacity. The remaining capacity was calculated in terms of the characteristic grain size (diameter for spheres, side length for tetrahedrons). The remaining capacity as a function of the thickness of the oxide layer and the grain size is illustrated in Fig. 6. The oxygen concentration for a $ZrV_{0.5}Ni_{1.5}$ sample exposed to air at room temperature, determined by X-ray photospectroscopy (XPS), decreased exponentially with depth. The half concentration length was approximately 30 Å with 1.5 oxygen atoms per AB_2 at this depth (AB_2 is the sum of all the metallic elements Zr+V+Ni in the alloy). This thickness of the oxide layer does not affect the storage capacity of some μm large particles.

The nickel compacted electrode showed the fastest activation and degradation as well. Activation may be better because of the hardness of nickel compared with copper. Nickel grains may produce or expand cracks in the alloy grains when the pellets are compressed. The creation of new cracks through the oxide layer of the alloy grains is also a possibility. Furthermore, the average nickel grains were smaller than those of copper. This would allow better electrical contact. The fast degradation of the nickel compacted electrode can be explained by the oxidation of nickel during discharge.

$$(Ni(OH)_2 + 2e^- \longleftrightarrow Ni + 2OH^- \text{ at } -0.76 \text{ V } vs. \text{ Hg/HgO/OH}^-)$$

The oxidation of the nickel powder increases poor grain-to-grain contact. Oxidation of the nickel grains together with oxidation of alloy grains explains the rapid degradation of the nickel compacted electrode.

The gold compacted electrode had a slow activation constant and a much lower maximum capacity than copper compacted electrodes. In contrast to nickel, gold is too soft for use as compacting material. Some of the alloy grains could have been pressed into the gold matrix and, therefore, they were never in contact with the electrolyte. The rate of degradation of the gold compacted electrode was between that of copper and nickel compacted electrodes, indicating that degradation was mainly due to corrosion of the alloy.

The platinum-coated carbon compacted electrode showed the poorest cycle-life curve. Carbon has a low electrical conductivity compared with copper or nickel and is a poor binding material. This was demonstrated by the fact that the internal resistance and the high rate dischargeability did not correlate with that of other electrodes.

The cobalt compacted electrode showed a very high capacity due to the formation of cobalt hydroxide and dissolution of $Co(OH)_2$ in the KOH electrolyte during

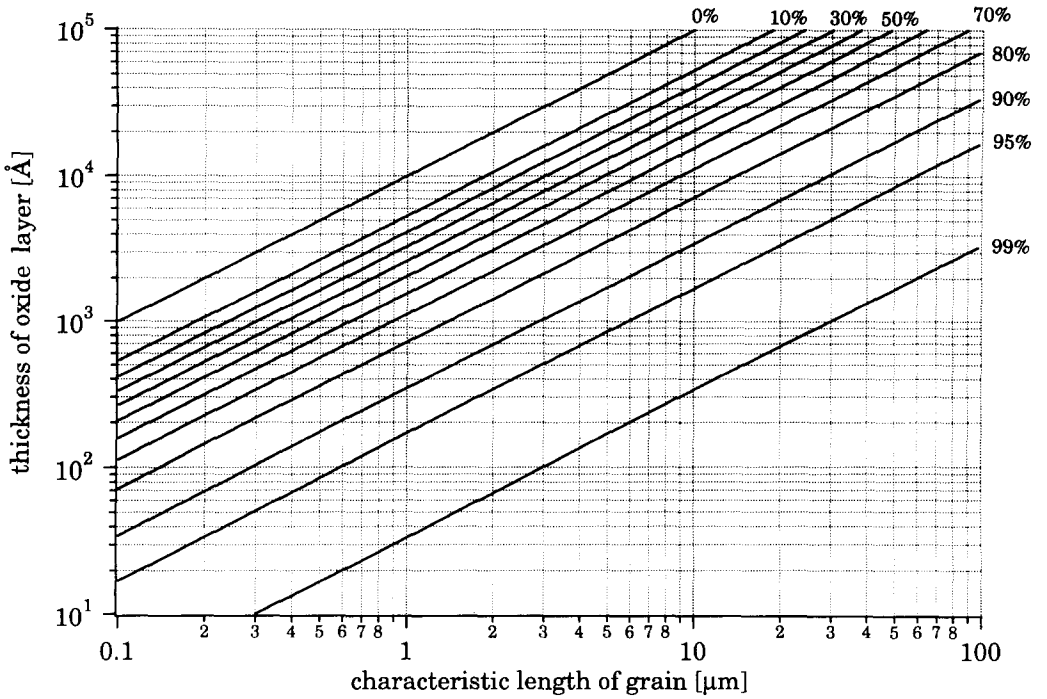

Fig. 6. Remaining capacity of alloy grains as a function of the thickness of oxide layer at the surface of the alloy grains and the characteristic length of grains (diameter for spheres, side length for tetrahedrons).

discharge.

$$(Co(OH)_2 + 2e^- \longleftrightarrow Co + 2OH^- \text{ at } -0.83 \text{ V } vs. \text{ Hg/HgO/OH}^-)$$

This partly reversible reaction produces theoretically an additional capacity of approximately 900 mA h g^{-1}. In other words, one cobalt atom has the same capacity as two hydrogen atoms. The discharge capacity of cobalt powder was measured experimentally and shown to be 200 mA h g^{-1} for more than 80 cycles. This discrepancy may be explained by the formation of passivating cobalt hydroxide on the metallic cobalt combined with the low dissolution rate of cobalt hydroxide in the electrolyte.

The ratio of the high to low rate discharge capacity has a limit at 83% (Fig. 2). We have found that the charge acceptance varies over a wide current range (up to 1 C, *i.e.* fully charged in 1 h) independent of the charge current. Freshly prepared electrodes are fully charged within the first 5 cycles [5]. The rate limiting difference between the charge and the discharge reaction lies at the metal surface/electrolyte interface. This is because the discharge of the $ZrV_{0.5}Ni_{1.5}$ in the gas phase is fast, indicating that diffusion of hydrogen in the bulk material is not the rate limiting step. Discharging 1 g of alloy involves the exchange of at least 0.4 ml of electrolyte (6 M KOH) or approximately twice the volume of the alloy. The porosity of our electrodes (20% alloy and 80% compacting material) was observed between 20 vol.% and 35 vol.%. This means the electrolyte in the electrode has to be fully exchanged at least once during discharge reaction. The charge reaction involves an exchange of only one tenth of the electrolyte compared with the discharge reaction. This is due to the concentration of water molecules which is ten times greater than the concentration of hydroxyl ions. In the pores the exchange of ions between the electrode and the electrolyte may be one reason for saturation of the high rate dischargeability as a function of the internal resistance of the electrode.

The potential after discharge of a nickel compacted electrode exactly paralleled the equilibrium potential curve during the first 30 cycles (activation). It can be assumed that after a few cycles the electrode is entirely charged and the discharge capacity is limited by a discharge barrier. With further cycles in the degradation part of the cycle-life curve, the potential after discharge remained constant while the discharge capacity decreased for high discharge current and for low discharge current as well. This constant potential shows that the remaining amount of hydrogen in the electrode after discharge is constant. It can be assumed that in the degradation part of the cycle-life curve, the loss of capacity is due to loss of hydrogen storage places and not due to a discharge barrier.

5. Conclusions

Compacting materials have a big influence on electrode performance. Using nickel as a compacting powder

gave the best activation results for the electrodes, while copper compacted electrodes showed the best cyclic stability. The amount of the compacting material also has an important effect on the internal resistance of the electrode, especially for ratios of alloy to compacting material higher than 25%.

Differences in electrode performance can be explained by oxidation stability, hardness of the grains and electrical conductivity of the compacting materials. Furthermore, the porosity of the electrodes has an important effect on performance due to the exchange of ions between the bulk electrolyte and the double layer at the alloy grain surface during charging and especially discharging of the electrode.

At this point the direct influence of compacting materials on the electron transfer reaction is not well known. However, the possibility exists that there is a catalytic effect at the grain boundaries between the alloy and the compacting metals.

Acknowledgment

Financial support was provided by the Bundesamt für Energiewirtschaft BEW (Swiss Department of Energy).

References

1 H. Ishikawa, K. Oguro, A. Kato, H. Suzuki and E. Ishii, *J. Less-Common Met., 107* (1985) 105.
2 S. Wakao, H. Sawa, H. Nakano, S. Chubachi and M. Abe, *J. Less-Common Met., 131* (1987) 311.
3 H. Sawa, M. Ohta, H. Nakano and S. Wakao, *Z. Phys. Chem. N.F., Bd. 164* (1989) 1527.
4 A. Züttel, F. Meli and L. Schlapbach, *J. Alloys Comp., 200* (1993) 157–163.
5 A. Züttel, F. Meli and L. Schlapbach, *J. Alloys Comp., 203* (1993) 235–241.
6 L. Schlapbach, *J. Less-Common Met., 89* (1983) 37.
7 R.C. Weast (ed.), *Handbook of Chemistry and Physics,* 57th edn., CRC Press, Boca Raton, 1976.